

Formation of Two-Dimensional Polarons that are Absent in Three-Dimensional Crystals

M. Muntwiler and X.-Y. Zhu*

Department of Chemistry, University of Minnesota, Minneapolis, Minnesota 55455, USA

(Received 12 January 2007; published 14 June 2007)

We report the direct time domain observation of a many-body process in a two-dimensional system: small polaron formation from the localization of a conduction band electron in NaCl thin films of unit cell thickness. Contrary to theoretical prediction for bulk NaCl crystal where an electron polaron does not exist, time-resolved two-photon photoemission reveals small polaron formation from delocalized conduction band electrons in crystalline NaCl thin films. The increased deformability and the reduced electronic bandwidth of a crystalline lattice in the thin film format are both responsible for the formation of small polarons that are absent in bulk solids.

DOI: 10.1103/PhysRevLett.98.246801

PACS numbers: 73.20.Mf, 78.67.-n

Electrons confined in two-dimensional systems, such as interfaces and ultrathin films, are central to low dimensional physics. The electronic structures of these materials are controlled by quantum confinement (in one direction) and are well known from extensive experimental and theoretical studies. In contrast, little is known about many-body processes, such as polaron formation, as a solid material reduces to a two-dimensional ultrathin film. Conceptually introduced decades ago [1,2], a small polaron, i.e., an electron or hole trapped in a distorted atomic structure, still challenges current theoretical models [3,4]. Exemplary cases are alkali halides which are used to illustrate electron polaron formation in standard textbooks, although theoretical studies predict that an electron polaron does not exist in crystalline alkali halides but a hole polaron does [3,4]. Here we show that, contrary to these predictions for a bulk crystal, localized polarons readily form from delocalized conduction band electrons in crystalline NaCl *thin films* supported on a metal surface. We use femtosecond time-resolved two-photon photoemission (TR-2PPE) spectroscopy to follow the formation and decay of small polarons by recording the energy and parallel dispersion of the transient electron en route to localization in real time. The present study establishes that the increased deformability and the reduced electronic band width of a crystalline lattice in the thin film format can lead to the formation of small polarons that are absent in bulk solids.

TR-2PPE is a pump-probe technique particularly useful for tracking interfacial electron dynamics [5]. In this approach, the first photon excites an electron from an occupied state (typically an occupied substrate band) into an unoccupied interfacial state. After a variable time delay, the second photon ionizes the electron for detection, as shown schematically in Fig. 1. In addition to monitoring the electron energy and population as a function of time, TR-2PPE also allows one to measure the parallel dispersion which is a measure of the extent of delocalization or localization of the electron wave function in the surface plane. TR-2PPE has been successfully applied in the past to probing localization dynamics of image states on adsorbate covered metal surfaces [6] and the solvation of elec-

trons in thin polar films [7,8]. The present study applies the technique for the first time to directly probe the dynamics of polaron formation in crystalline solid thin films from conduction band electrons.

All experiments are carried out in an ultrahigh vacuum system described elsewhere [9]. NaCl thin films are depos-

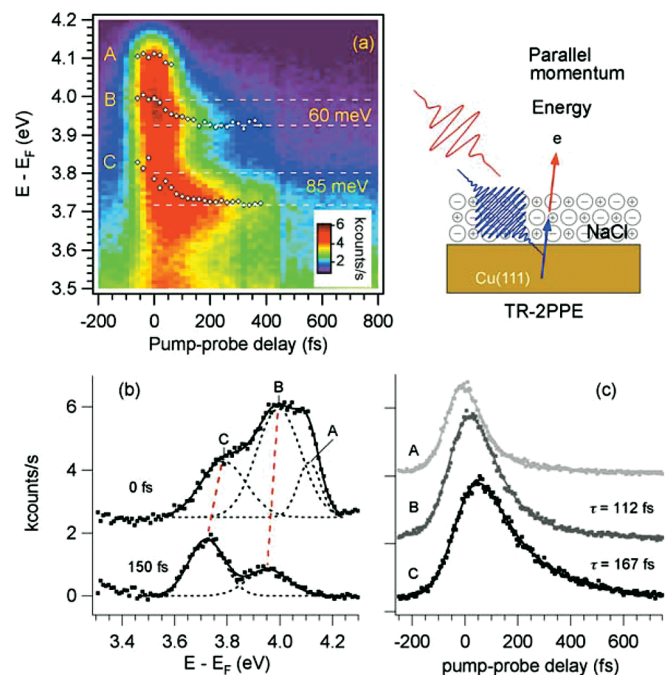


FIG. 1 (color). (a) Two-dimensional pseudocolor representation of 2PPE spectra as a function of pump-probe delay for 3 ML NaCl/Cu(111). The energy scale corresponds to intermediate state energy referenced to the Fermi level. Peak positions are shown as white circles. (b) Two vertical cuts in (a) at the indicated pump-probe delay times. The spectra are offset with background removed for clarity. Dots are experimental data and the solid lines are overall fits from the individual Gaussian components (dashed curves). (c) Energy-integrated peak intensities as a function of pump-probe delay. Solid lines are fits to a rate equation model which yields the indicated lifetimes. A schematic of the 2PPE experiment is also shown.

ited on a clean Cu(111) surface heated to 335 K from a Knudsen cell. Film thickness is calibrated by thermal desorption spectroscopy and low energy electron diffraction. NaCl vapor deposited on Cu(111) forms a crystalline cubic lattice, with (100) orientation, which is incommensurate with the substrate [10,11]. There are three rotational domains due to substrate symmetry; each single crystal domain has lateral sizes up to $\sim 1 \mu\text{m}$. We study NaCl film thicknesses of 2–5 monolayers (ML). All TR-2PPE experiments are carried out at a sample temperature of 105 K. In the experiment, the third harmonic ($h\nu_1 = 4.180 \text{ eV}$) and the fundamental ($h\nu_2 = 1.393 \text{ eV}$) output of a femto-second Ti:sapphire oscillator are used as pump and probe pulses, respectively, and photoemitted electrons are detected by a hemispherical electron energy analyzer. A laser pulse width of $\sim 100 \text{ fs}$ is determined from cross-correlation measurement on the occupied surface state on clean Cu(111). Except for dispersion measurements where the angle of detection is varied, all TR-2PPE measurements were carried out with the sample surface normal to the electron detector.

The pseudocolor plot in Fig. 1(a) shows 2PPE intensity versus electron energy and pump-probe delay for 3 ML NaCl on Cu(111). Each vertical cut corresponds to a 2PPE spectrum at a particular pump-probe delay Δt , as shown for $\Delta t = 0$, and 150 fs in 1(b). Each horizontal cut is a cross-correlation curve at a particular electron energy and gives the relaxation of an electron due to energy and population decays. For $\Delta t = 0 \text{ fs}$, the 2PPE spectrum shows three peaks above 3.7 eV. The highest one (A) at 4.10 eV is the image state due to small patches of clean Cu(111) [12]. It has a short lifetime ($< 20 \text{ fs}$) and disappears at higher NaCl coverages. The two peaks (B and C) at lower energies (~ 3.98 and $\sim 3.78 \text{ eV}$) show clearly measurable lifetimes. We assign them to the conduction band of the NaCl thin film for the following reasons: (i) These are not commonly seen image-potential states because the adsorption of an insulating overlayer has little effect, indicating the electron wave function is predominantly confined to the NaCl thin film (see Fig. 2); (ii) the band gap of NaCl is 8.5–9 eV [13,14]. Since there is little chemical interaction between NaCl and the Cu(111) substrate [11], we can assume a midgap alignment as found for NaCl on Ge [15], which puts the NaCl conduction band minimum at $\sim 4.3 \text{ eV}$ above the Fermi level. This estimated position is further stabilized on the metal surface by the image potential. It is known that a surface-related band within 1 eV below the conduction band minimum (CBM) splits off the bulk conduction band in NaCl crystal [16,17]. Thus, we can assign peak B to the conduction band of the NaCl thin film and peak C to its split-off, i.e., a surface conduction band. (iii) At $\Delta t = 0 \text{ fs}$, the two states show free-electron-like parallel dispersions with effective electron masses close to those of the bulk and surface NaCl conduction bands (see Fig. 3). (iv) We find that deliberately increasing the defect density in NaCl by using lower substrate temperature during thin film growth or by electron irradiation leads to a

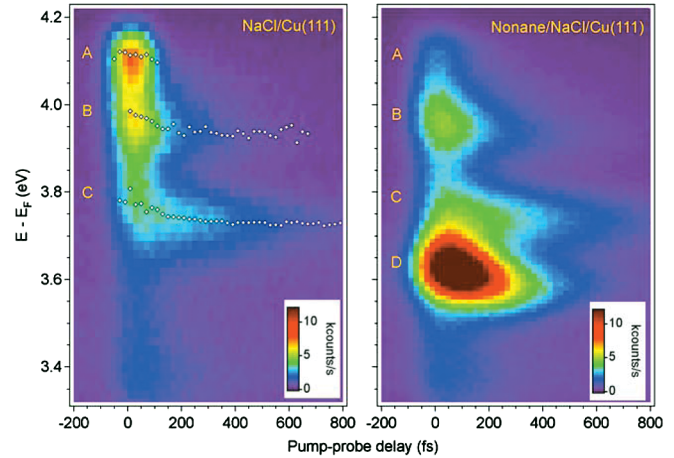


FIG. 2 (color). A comparison of time-resolved 2PPE spectra (shown in pseudocolor representation) for NaCl/Cu(111) (left) and the same surface with one monolayer of nonane adsorbed on top. The thickness of the NaCl film is between 2 and 3 ML. Peak positions are shown as open circles in the left panel.

disappearance of peaks B and C. This likely results from the decreased probability of photoexcitation from occupied metal bands into the NaCl conduction band as crystallinity of the NaCl thin film degrades.

To identify the spatial localization (inside or outside of the NaCl film) of the states observed in 2PPE spectra, we compare measurements on NaCl thin films with and without a dielectric overlayer, Fig. 2. Peaks B and C are not affected by the adsorption of the overlayer, indicating that the electron wave function is confined to the NaCl film or the NaCl/Cu interface. In contrast, image state wave functions would be significantly modified by an overlayer with negative electron affinity [6]. This is evident for peak A which disappears. On the other hand, a new and intense peak D appears which is likely an imagelike state associated with the nonane overlayer or the nonane-NaCl interface. Its energetic position may be explained by coupling to the surface or conduction band of NaCl, as implied by the dielectric continuum model [18]. It is stabilized by 30 meV in 200 fs due to small polaron formation in the alkane layer, as observed before for alkane/Ag(111) [6].

The most significant finding from TR-2PPE is the time-dependent energy relaxation of peaks B and C. The energetic positions of the two bands decrease by 60 ± 10 and $85 \pm 10 \text{ meV}$, respectively, with increasing pump-probe delay time, as shown in Figs. 1(a) and 1(b). Fitting the time-dependent decay in peak positions to single exponentials gives energy relaxation lifetimes of $\tau_e = 75 \pm 11$ and $95 \pm 11 \text{ fs}$ for peaks B and C, respectively. We attribute the observed energy relaxation to the formation of small polarons from conduction and surface bands of the NaCl thin film. This interpretation is verified by dispersion measurements: a delocalized band electron should show free-electron-like dispersion while a localized polaron appears as a flat band. Figure 3 shows parallel dispersions measured at $\Delta t = 0, 125, 400 \text{ fs}$ pump-probe delays. For

$\Delta t = 0$ fs, we also present a monochromatic measurement, Fig. 3(a), in which the conduction band is well resolved from the image state. Parallel dispersions from the conduction and the surface bands at $\Delta t = 0$ fs, 3(a) and 3(b), are indeed free-electron-like with fits to

$$E = E_o + \frac{\hbar^2 k_{\parallel}^2}{2m_{\text{eff}}} \quad (1)$$

giving effective electron masses of $m_{\text{eff}} = 0.8 \pm 0.1m_e$ and $0.6 \pm 0.1m_e$ for the conduction band and the surface band, respectively. Here, E_o is the band bottom and m_e is the free-electron mass. The observed effective electron masses are slightly higher than those of conduction and surface bands of bulk crystalline NaCl(100) [13,17,19], as expected from the reduced bandwidth in the thin film format. When Δt is increased to 125 fs, both bands significantly flatten with effective electron masses of $m_{\text{eff}} = 3.2 \pm 1.5m_e$ and $3.9 \pm 1.5m_e$ for the conduction band and the surface band, respectively. At $\Delta t = 400$ fs, Fig. 3(d), both bands are essentially flat, as expected for localized small polarons.

The energy of charge carrier self-trapping (E_{ST}) in a crystalline solid can be estimated from three factors [4]:

$$E_{\text{ST}} = E_{\text{pol}} + E_{\text{loc}} + E_{\text{bond}}, \quad (2)$$

where E_{pol} is the energy gain from polarization of the lattice surrounding the charge carrier, E_{loc} is the energetic penalty associated with going from a delocalized band state to a localized trap state and can be approximated by half of the band width ($E_{\text{loc}} \approx 0.5\Delta E$), E_{bond} is specific to some crystalline solids, such as alkali halides, where local lattice deformation leads directly to chemical bond formation, e.g., Cl-Cl^- for a self-trapped hole or Na-Na^+ for a self-trapped electron in NaCl. The valence and conduction bandwidths of NaCl are $\Delta E_{\text{VB}} = 2.4$ eV and $\Delta E_{\text{CB}} = 5.0$ eV [13], respectively, and the bond energies are $E_{\text{bond}} = -1.2$ eV for Cl-Cl^- [20] and -1.0 eV for Na-Na^+ [21]. The hole polaron is stable in NaCl and the

hole self-trapping energy E_{ST} is estimated from the hole diffusion barrier [22] to be -0.4 eV or lower [23]. Taking the limiting value and Eq. (2) gives a hole polarization energy of $E_{\text{pol}} \approx -0.4$ eV; for comparison, E_{pol} for a hole in KCl is -0.5 eV [4]. The electron polarization energy is believed to be similar to that of the hole. Thus, we can estimate an electron self-trapping energy of $E_{\text{ST}} \approx 1.1$ eV, which means that the electron polaron is unstable in the bulk NaCl crystal. For comparison, a positronium polaron in bulk NaCl or other alkali halides is metastable, with the self-trapping energy slightly positive (0.01–0.1 eV) [24].

Why does an electron polaron become stable in thin NaCl films? We believe the main reason is the increase in the magnitude of E_{pol} in the thin film format because it is more deformable than the bulk crystal. A recent scanning tunneling microscopy study shows that an anionic Au^- adatom can be stabilized on the NaCl/Cu(111) surface; density functional calculation attributes this to the deformation of the local ionic lattice which stabilizes the adatom by as much as 1.0 eV [25]. An additional contribution is the narrower bandwidth. Within the tight-binding approximation, the bandwidth of a cubic NaCl film with thickness on the order of the unit cell is 2/3 of that of the bulk due to the reduced number of neighboring sites. If we approximate E_{pol} by that calculated for Au^- on NaCl [25], we can estimate an electron polaron self-trapping energy in the NaCl thin film: $E_{\text{ST}} \approx -0.3$ eV. Thus an electron polaron becomes stable in a NaCl thin film. The magnitude of this estimate is a factor 3–4 larger than the values observed in our TR-2PPE measurements. However, a more accurate calculation is hampered by limitations of current theoretical methods [23]. Note that for an ultrathin NaCl film on a metal surface, a conduction band electron or a polaron also experiences stabilization due to the image potential, but this has little effect on localization due to the delocalized nature of the image potential in the surface plane.

We consider two dynamic processes. The first dynamic process is small polaron formation following electron injection into the conduction and surface bands of the NaCl

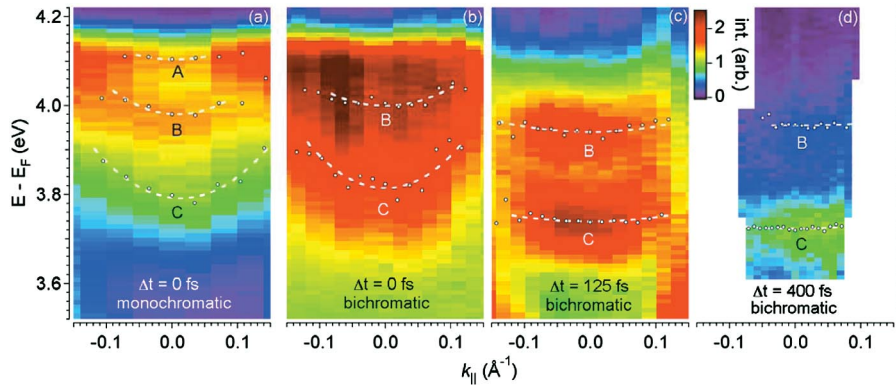


FIG. 3 (color). Angle-resolved 2PPE spectra (shown in pseudocolor representation) for 3–4 ML NaCl on Cu(111) at pump-probe delay times of (a) $\Delta t = 0$ fs, (b) $\Delta t = 0$ fs, (c) $\Delta t = 125$ fs, and (d) $\Delta t = 400$ fs. (a) was from monochromatic measurement ($h\nu_1 = h\nu_2 = 4.18$ eV) while (b)–(d) were from bichromatic measurements ($h\nu_1 = 4.16$ eV; $h\nu_2 = 1.39$ eV). The peak positions (white dots) versus k_{\parallel} give parallel dispersions. The dashed white curves are fits to the free-electron-like dispersion in Eq. (1).

thin film. The time-dependent decay in electron energies [peak positions in Fig. 1(a)] gives small polaron formation rate constants of $1/\tau_e = (1.3 \pm 0.2) \times 10^{13}$ and $(1.1 \pm 0.2) \times 10^{13} \text{ s}^{-1}$ for the conduction and surface band, respectively. These rate constants are within the frequency ranges defined by the phonon dispersions $((0-5) \times 10^{13} \text{ s}^{-1})$ in NaCl crystals [26]. Thus, the rate of small polaron formation is determined by the rate of lattice distortion. The second dynamic process is the relaxation of the excited electron. For an ultrathin film of NaCl on the metal surface, the most efficient relaxation pathway is electron transfer from NaCl to the metal substrate. This is reflected in the time-dependent decrease in electron population. To focus on the interfacial electron transfer process, we have integrated the 2PPE intensity within an energy window encompassing the energy relaxation. The results are shown as a function of pump-probe delay in Fig. 1(c). The solid lines are fits to a rate equation model [9] which gives the indicated lifetimes. Note that the image state lifetime (curve A) is too short to be resolved and the symmetric cross-correlation curve essentially reflects the laser pulses used. For the conduction and surface bands, the asymmetric cross-correlation curves, B and C, can be well described by rate equation fits corresponding to lifetimes of $\tau_p = 110 \pm 20$ and 170 ± 20 fs for the conduction band and the surface band, respectively. The longer lifetime in the surface band than that in the conduction band can be accounted for by the following argument. Both the CBM and the surface band minimum (SBM) of the NaCl(100) film are located within the projected band gap of the Cu(111) surface, but the CBM is closer to the upper band edge (4.2 eV above the Fermi level) [12] than is the SBM. As a result, the electron wave function of the former couples more strongly to the metal substrate, leading to a shorter lifetime.

We have carried out TR-2PPE measurements for film thicknesses of 2–5 ML. Results similar to those in Fig. 1 are found in all cases. We do not see significant differences in the dynamics of small polarons for different film thicknesses. The probability density of an electron wave function in the conduction or surface band of the NaCl thin film is attracted to the Cu(111) surface due to the presence of the metal image potential, thus minimizing the effect of increased film thickness. In addition, NaCl(100) is known to grow in the form of large domains (approximately micrometers) of bilayers [11,25] but growth beyond the bilayer leads to small islands. Photoemission from the bilayer in contact with the Cu(111) surface is expected to dominate the 2PPE signal because the rate of photoinduced electron injection from the metal surface into the adsorbate layer is determined by electronic coupling at the interface [27].

The results presented here establish the formation in thin films of small polarons that are absent in bulk crystalline solids. This is another manifestation of new physical properties that emerge as physical sizes (in one of the three

dimensions in the present case) decrease to the nanometer scale.

This work was supported by the U.S. National Science Foundation MRSEC Program under Grant No. DMR 0212302. Partial support from the U.S. National Science Foundation Grant No. DMR 0238307 is also acknowledged.

*Email address: zhu@chem.umn.edu

- [1] L. Landau, Phys. Z. Sowjetunion **3**, 664 (1933).
- [2] T. Holstein, Ann. Phys. (N.Y.) **8**, 343 (1959).
- [3] A. L. Shluger and A. M. Stoneham, J. Phys. Condens. Matter **5**, 3049 (1993).
- [4] R. T. Williams and K. S. Song, J. Phys. Chem. Solids **51**, 679 (1990).
- [5] P. Szymanski, S. Garrett-Roe, and C. B. Harris, Prog. Surf. Sci. **78**, 1 (2005).
- [6] N. H. Ge, C. M. Wong, R. L. Lingle, Jr., J. D. McNeill, K. J. Gaffney, and C. B. Harris Science **279**, 202 (1998).
- [7] C. Gahl, U. Bovensiepen, C. Frischkorn, and M. Wolf, Phys. Rev. Lett. **89**, 107402 (2002).
- [8] A. D. Miller, I. Bezel, K. J. Gaffney, S. Garrett-Roe, S. H. Liu, P. Szymanski, and C. B. Harris, Science **297**, 1163 (2002).
- [9] C. Lindstrom, D. Quinn, and X.-Y. Zhu, J. Chem. Phys. **122**, 124714 (2005).
- [10] R. Bennowitz, V. Barwich, M. Bammerlin, C. Loppacher, M. Guggisberg, A. Baratoff, E. Meyer, and H. Güntherodt, Surf. Sci. **438**, 289 (1999).
- [11] J. Repp, G. Meyer, and K.-H. Rieder, Phys. Rev. Lett. **92**, 036803 (2004).
- [12] P. M. Echenique, R. Berndt, E. V. Chulkov, Th. Fauster, A. Goldmann, and U. Höfer, Surf. Sci. Rep. **52**, 219 (2004).
- [13] F.-J. Himpsel and W. Steinmann, Phys. Rev. B **17**, 2537 (1978).
- [14] F. Bechstedt, K. Seino, P. H. Hahn, and W. G. Schmidt, Phys. Rev. B **72**, 245114 (2005).
- [15] U. Barjenbruch, S. Fölsch, and M. Henzler, Surf. Sci. **211/212**, 749 (1989).
- [16] J. D. Levine and P. Mark, Phys. Rev. **144**, 751 (1966).
- [17] W. Kisiel and B. Stankiewicz, Surf. Sci. **231**, 32 (1990).
- [18] C. B. Harris, N.-H. Ge, R. L. Lingle, Jr., J. D. McNeil, and C. M. Wong, Annu. Rev. Phys. Chem. **48**, 711 (1997).
- [19] Z. Y. Evseev, Sov. Phys. Solid State **5**, 2345 (1963).
- [20] T. L. Gilbert and A. C. Wahl, J. Chem. Phys. **55**, 5247 (1971).
- [21] K. K. Verma, J. T. Bahns, A. R. Rajaei-Rizi, W. C. Stwalley, and W. T. Zemke, J. Chem. Phys. **78**, 3599 (1983).
- [22] K. Tanimura and N. Itoh, J. Phys. Chem. Solids **42**, 901 (1981).
- [23] J. L. Gavartin, P. V. Sushko, and A. L. Shluger, Phys. Rev. B **67**, 035108 (2003).
- [24] I. V. Bondarev, Phys. Rev. B **58**, 12011 (1998).
- [25] J. Repp, G. Meyer, F. E. Olsson, and M. Persson, Science **305**, 493 (2004).
- [26] G. Raunio, L. Almqvist, and R. Stedman, Phys. Rev. **178**, 1496 (1969).
- [27] C. D. Lindstrom and X.-Y. Zhu, Chem. Rev. **106**, 4281 (2006).